IEICE Proceeding Series

Non-Uniform Arrays of bi-SQUIDs

Patrick Longhini, Visarath In, Antonio Palacios, Susan Berggren, Oleg A. Mukhanov, Georgy Prokopenko, Anna Leese de Escobar, Benjamin Taylor, Marcio C. De Andrade, Martin Nisenof

Vol. 2 pp. 118-121
Publication Date: 2014/03/18
Online ISSN: 2188-5079

Non-Uniform Arrays of bi-SQUIDs

Patrick Longhini† Visarath In† Antonio Palacios‡ Susan Berggren†
Oleg A. Mukhanov♭ Georgy Prokopenko♭ Anna Leese de Escobar†
Benjamin Taylor† Marcio C. De Andrade† and Martin Nisenoff♣

†Space and Naval Warfare Systems Center
53560 Hull Street, San Diego, CA 92152-5001, USA
‡Nonlinear Dynamical Systems Group, Department of Mathematics
San Diego State University, San Diego, CA 92182, USA.
♭ HYPRES, Inc., 175 Clearbrook Road, Elmsford, NY 10523, USA
♣ M. Nisenoff Associates, 1201 Yale Place, Suite #1004,Minneapolis MN 55403 USA.
Email: patrick.longhini@navy.mil visarath@spawar.navy.mil

Abstract—Multi-loop arrays of Josephson Junctions (JJ) with non-uniform area distributions, which are known as Superconducting Quantum Interference Filters (SQIF), are the most highly sensitive sensors of changes in applied magnetic field as well as the absolute magnitude of magnetic fields. The non-uniformity in the loop inductances allows the array to produce a unique collective voltage response that has a pronounced single peak with a large voltage swing around zero magnetic field. To obtain high linear dynamic range, which is critical for a wide variety of applications, the linearity of the slope of the anti-peak response must be improved. We propose a novel scheme for enhancing linearity - a new configuration combining the SQIF array concept with the recently introduced bi-SQUID configuration, in which each individual SQUID loop is made up of three JJs as opposed to using two JJs per loop in standard dc SQUIDs. The anti-peak linearity and size can be optimized by varying the critical current that circulates through the additional junction of each bi-SQUID. We show, computationally, that the additional junction offers a viable linearization method for optimizing the voltage response and dynamic range of SQIF arrays. We have realized the SQIF arrays based on bi-SQUID cells and present experimental results which verify the numerical results.

1. Introduction

It is well known that one of the most sensitive magnetic field devices is the Superconductive Quantum Interference Device (SQUID), and is used for wide range of applications including biology, medicine, geology, systems for semiconductor circuit diagnostics, security MRI and even cosmology research [1–6]. In recent years, arrays of coupled oscillators have been considered as a general mechanism for improving signal detection and amplification [7–9]. Indeed, theoretical [10, 11] and experimental studies [12] have shown that arrays of SQUIDs can yield comparable improvements in signal output, relative to background noise, over those of a single device. A peculiar configuration that has gained considerable attention among the physics and engineering community is that of multi-loop arrays of JJs with non-uniformly distributed loop areas. Typically, each loop contains two JJs, i.e., a standard dc SQUID, but their size vary from loop to loop. These types of unconventional geometric structures of JJs are known to exhibit a magnetic flux dependent voltage response $V(\varphi_e)$, where φ_e denotes an external magnetic flux normalized by the quantum flux, that has a pronounced single peak with a large voltage swing at zero magnetic field. The potential high dynamic range and linearity of the "anti-peak" voltage response render the array an ideal detector of absolute strength of external magnetic fields, so these arrays are also commonly known as Superconducting Quantum Interference Filters (SQIFs). Since it was theoretically proposed [13, 14] and experimentally demonstrated for the first time [15–17] the SQIF concept is investigated and exploited by a continuously growing number of groups.

In this paper, we investigate a different approach, one that involves a change in the configuration of the array. Mainly, each individual array cell will now contain three JJs as oppose to the standard practice of two JJs per loop. These new type of SQUIDs are also known as bi-SQUIDs [19] because the additional junction and main inductance form an additional single-junction SQUID. We demonstrate, numerically and experimentally, that bi-SQUIDs can be integrated into non-uniform arrays, bi-SQUID-based SQIFs, and that they offer a novel linearization method for maximizing its voltage response and dynamic range.

2. Background

2.1. The DC bi-SQUID

The dc bi-SQUID was originally introduced by Kornev *et al.* [19–21] as a modified version of a conventional SQUID device but with the ability to produce a highly linear voltage response. Figure 1(top) shows a circuit diagram of the proposed bi-SQUID device with the individ-

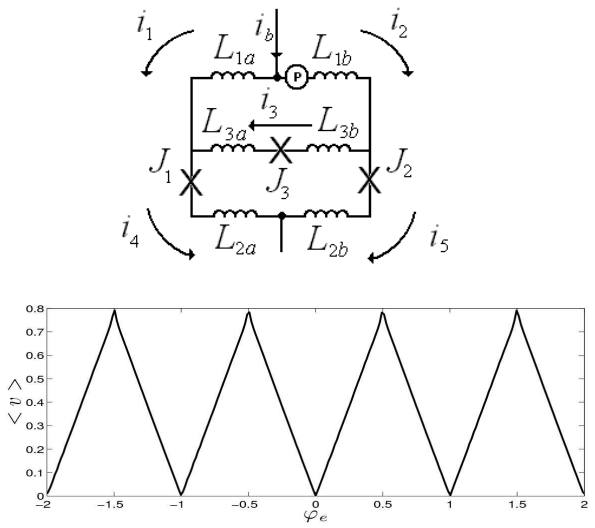

Figure 1: (Top) Circuit representation of a DC bi-SQUID device. 'P' is a phase source that accounts for the phase shift due to the external magnetic flux φ_e, with (bottom) its time-averaged voltage response between the two junctions, as a function of the normalized external magnetic flux φ_e.

ual inductances, L_{ja} and L_{jb}, where $j = 1, 2, 3$. The third junction, when combined with the main inductance in the loop, acts as a single-junction SQUID thus leading to a combined bi-SQUID system. More importantly, the works in [19–21] demonstrate that tuning of the nonlinear inductance, through the critical current of the junctions, can lead to significant improvements in the linearity of the $V(\varphi_e)$ curve.

Assuming identical junctions, leads to the following governing equations for the phase dynamics:

$$A\dot{\boldsymbol{\varphi}} = B\boldsymbol{\varphi} + C + Dsin(\boldsymbol{\varphi}) \tag{1}$$

with

$$A = \begin{bmatrix} (L_1 + L_{2a}) & -L_{2b} & -L_1 \\ L_{2a} & -(L_1 + L_{2b}) & -L_1 \\ L_{2a} & -L_{2b} & -(L_{3a} + L_{3b}) \end{bmatrix} \tag{2}$$

and

$$B = \begin{bmatrix} -1 & 1 & 0 \\ -1 & 1 & 0 \\ 1 & 1 & -1 \end{bmatrix} \qquad C = \begin{bmatrix} L_{1b}i_b + \boldsymbol{\varphi_e} \\ L_{1a}i_b + \boldsymbol{\varphi_e} \\ 0 \end{bmatrix} \tag{3}$$

$$D = -A \begin{bmatrix} 0 & 0 & i_{c3} \\ 0 & 0 & i_{c3} \\ 0 & 0 & i_{c3} \end{bmatrix} \tag{4}$$

where, $\boldsymbol{\varphi_e} = 2\pi\varphi_e a_n$, $\boldsymbol{\varphi} = (\varphi_1, \varphi_2, \varphi_3)$ are the phases on each of the junctions J_n, $n = 1, 2, 3$, $L_1 = (L_{1a} + L_{1b})$, $i_{c3} = I_{c3}/I_c$, is the normalized critical current across the third junction J_3, $I_{c1} = I_{c2} = I_c$, a_n is a nonlinearity parameter related to the loop size between J_1 and J_2, and $\dot{()}$ denotes differentiation with respect to the normalized time $\tau = \omega_c t$, $\omega_c = 2\pi V_c/\Phi_0$, $V_c = I_c R_N$. Figure 1(bottom) illustrates the average voltage response of a bi-SQUID device obtained numerically by integrating Eqs. (1) and then calculating $< v >$ through

$$< v >= \frac{1}{T}\int_0^T \left(\frac{\dot{\varphi}_1 + \dot{\varphi}_2}{2}\right) \tag{5}$$

with the following parameters: $i_b = 2$, $a_n = 1$, $L_{1a} = L_{1b} = 0.27$, $L_{2a} = L_{2b} = 0.24$, $L_{3a} = L_{3b} = 0.3$. The voltage response of the bi-SQUID is significantly more linear than that of the conventional SQUID.

In Fig. 2 we now explore the effects of changing the nonlinear inductance on the linearity of the average voltage response curve $V(\varphi_e)$. At small magnitudes of the critical current i_{c3}, the shape of the voltage response curve closely resembles that of a conventional SQUID. As the parameter i_{c3} increases, the transfer function linearity increases while the voltage response approaches a triangular shape. For larger values of the $i_{c3} > 1.0$ parameter, the voltage response curve develops a cusp which results in a hysteresis loop and a decrease in linearity, as shown in Fig. 2(bottom). Thus, there appears to be an optimal value of the critical current i_{c3}, located at intermediate magnitudes, where a bi-SQUID device can generate the most linear voltage response.

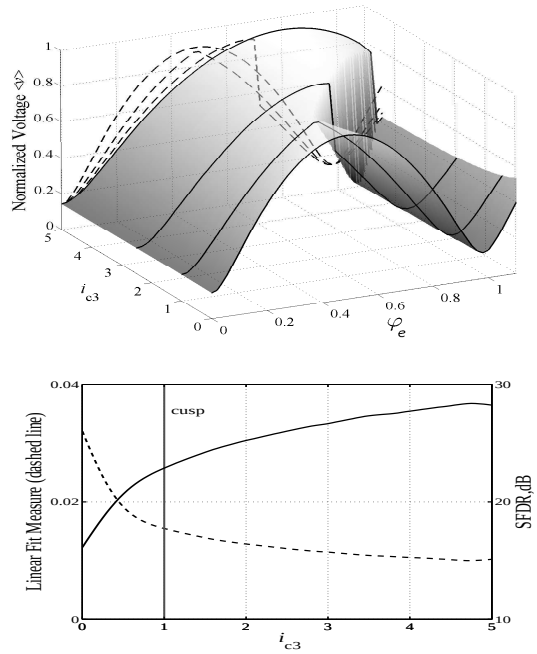

Figure 2: (Top) Numerical simulations of the voltage response of a single bi-SQUID. (Bottom) Linearity test via linear fitting error and through calculations of Spur Free Dynamic Range (SFDR).

Experiments with non-uniform multi-loop serial arrays of conventional SQUIDs have shown that the voltage swing

of the response curve $V(\varphi_e)$ increases proportionally to the number of SQUIDs in the array.

3. Serial bi-SQUID Array

Generically, a serial array of N SQUIDs is able to yield a significantly higher output power than a single SQUID. In particular, dynamic range is known to increase as $N^{1/2}$ in the presence of thermal noise [18]. Thus, in principle, serial arrays of bi-SQUIDs can be implemented to produce a voltage anti-peak response with increased dynamic range and improved voltage linearity. Indeed, the motivation of this work is to build a (serial) SQIF [13–16] array consisting of bi-SQUIDs. To pursue this goal, we consider in this section a serial array of N bi-SQUIDs, designed as is shown in Fig. 3.

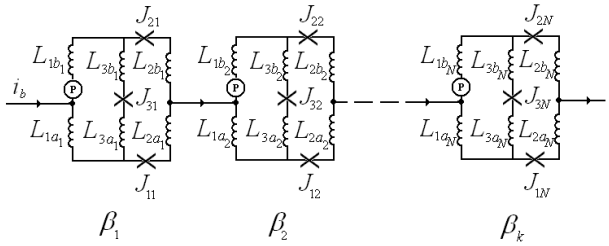

Figure 3: Circuit representation of an array of bi-SQUID devices connected in series. 'P' related to external magnetic flux φ_e.

The derivation of the equations governing the phase across each of the junctions is described by the following system of differential equations.

$$A_i\dot{\boldsymbol{\varphi}}_{\boldsymbol{i}} = B\boldsymbol{\varphi}_{\boldsymbol{i}} + C_i + D_i sin(\boldsymbol{\varphi}_{\boldsymbol{i}}) + M\Phi_i \qquad (6)$$

where $\boldsymbol{\varphi} = \varphi_{i,j}$ are the phases on each of the junctions $J_{i,j}$, $i = 1..N$, $j = 1, 2, 3$, $L_{1,i} = (L_{1a,i} + L_{1b,i})$, $a_{n,i}$ is a parameter related to the loop size between $J_{i,1}$ and $J_{i,2}$, and M is the coupling strength for the phase interaction Φ_i between nearest neighbors — one neighbor for the edge elements, two for the inner elements — according to

$$\Phi_i = a^{-1}_{n,i+1}(\varphi_{i+1,1} - \varphi_{i+1,2} - \boldsymbol{\varphi_e}) - a^{-1}_{n,i-1}(\varphi_{i-1,1} - \varphi_{i-1,2} - \boldsymbol{\varphi_e}), \qquad (7)$$

where, $a_{n,0} = a_{n,N+1} = 0$, $\boldsymbol{\varphi_e} = 2\pi\varphi_e a_{n,i}$, i_b is the bias current, $i_{c3} = I_{c3}/I_c$ is the normalized critical current of the third junction J_3 in each bi-SQUID cell, $a_{n,i}$ is the nonlinearity parameter related to the ith bi-SQUID loop. For simplicity, in this work we assume all inductances to be identical throughout the array. The main differences from the single bi-SQUID are the mutual inductances between elements.

Numerical simulations of Eq.(6) were carried out to explore, computationally, the voltage response of the serial array as a function of the external field φ_e and the critical current i_{c3}. Different distributions of loop sizes were investigated for each array, including: linear, Gaussian, exponential, logarithmic, and equal size.The Gaussian was only slightly better and it would be redundant to display results on the other distributions. From now on in the paper we are assuming that the distribution of loop sizes is Gaussian. Figure 4(a) shows the results of the simulations for a specific array with $N = 20$ bi-SQUID loops with loop sizes that vary according to a Gaussian distribution.

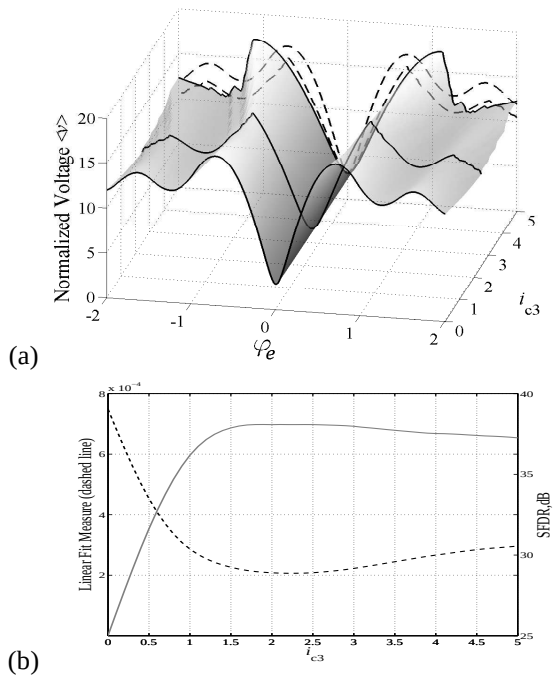

Figure 4: Numerical: (a) voltage response of a non-uniform serial bi-SQUID array ($N = 20$) (b) Linearity test (dashed line) via linear fitting error of N equals 20 bi-SQUID devices and corresponding SFDR (solid line).

Figure 4(b) shows the results of the linear fitting and SFDR. Indeed, the error in the linear fitting decreases as i_{c3} increases thus indicating an increase in the linearity of the voltage output. The increase in linearity is similar to what was observed previously in a single bi-SQUID, see Fig. 2, except that now the voltage output does not develop a hysteresis loop so that the linearity does not decrease for larger values of the critical current. Instead, there appears to be a threshold value of the critical current i_{c3} beyond which the linearity remains unchanged as is shown in Fig. 4(b).

4. Design and Fabrication

We have designed various configurations of bi-SQUID SQIF arrays in order to study various different layout configurations, junction damping, and coupling schemes. Figure 5(a,b) shows fabricated chips microphotographs of representative chips, e.g., a set of two different designs of a

256 and 1315 serial bi-SQUID-cell arrays. Figure 5(c,d) shows the measured flux-voltage characteristics of the respective serial bi-SQUID SQIF arrays.

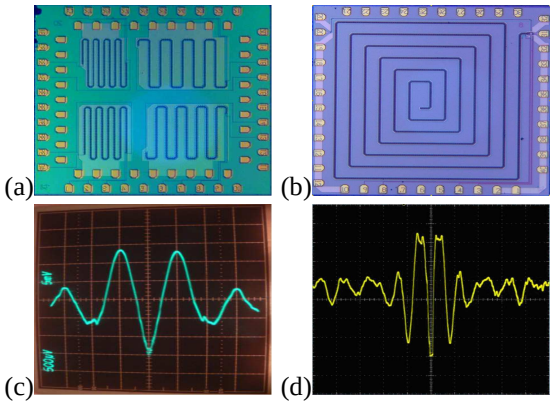

Figure 5: Microphotographs of the fabricated bi-SQUID-SQIFs integrated on 5 mm x 5 mm chips with corresponding measured flux-voltage characteristics of bi-SQUID SQIF arrays: (a,c) a serial 256 bi-SQUID array. (b,d) Serial spiral 1315-cell array.

Experimental measurements shown in Figure 5 confirm that the collective voltage output exhibits a pronounced single peak with a large voltage swing about zero magnetic flux. It also shows that bi-SQUIDs can be integrated into SQIF arrays and exhibit a linear response as predicted by results of modeling and simulations.

5. Conclusion

We have studied, analytically, computationally, and experimentally, the behavior of non-uniform area in multi-loop arrays of Josephson Junctions, also known as Superconducting Quantum Interference Filters. Analytically, we used basic circuit laws to derive model equations for the phase across each of the junction. Numerical simulations of the model equations revealed that the collective voltage output exhibits a pronounced single peak with a large voltage swing about zero magnetic flux. The shape of the anti-peak is due, mainly, to the non-uniformity of the multi-loop structure while its linearity appears to be directly correlated to parameter i_{c3}. The Gaussian distribution of loop sizes were used in a serial array which produced a clear linear response around the anti-peak. Various configurations of serial and parallel arrays of bi-SQUIDs were designed, fabricated, and tested. Note that in this paper only the serial was reported. The test results validated the theoretical findings: a serial array of bi-SQUIDs with loop sizes spread according to a Gaussian distribution produces a highly linear anti-peak voltage response. The linearity and size of the anti-peak in the serial bi-SQUID array can be optimized by changing the critical current through the third junction of each bi-SQUID element and by changing the number of loops. We anticipate that both serial and parallel bi-SQUID SQIF arrays can be integrated into a two-dimensional (2D) array structure to deliver superior linearity at appropriate impedance.

Acknowledgments

We gratefully acknowledge support from the Tactical SIGINT Technology Program N66001-08-D-0154. Office of Naval Research (ONR), Code 30,

References

[1] R. L . Fagaly, *Rev. Sci. Instrum.* **77**, 101101 (2006).

[2] L. E. Fong, J. R. Holzer, et al. *Rev. Sci. Instrum.* **76**, 053703 (2005).

[3] O. Hahneiser, S. Kohlsmann, et al. *Bioelectrochem. Bioenerg.*, **37**, 51, (1995).

[4] Y. Machitani, N. Kasai, et al. *IEEE Trans. Appl. Supercond.* **13** 763, (2003).

[5] P. Schmidt, D. Clark, et al. *Explor. Geophys.*, **35**, 297 (2004).

[6] Andreas Chwala, Ronny Stolz, et al. SEG Expanded Abstracts **29**, 779 (2010).

[7] D.G. Aronson, M. Golubitsky, and M. Krupa, *Nonlinearity* **4** 861, (1991).

[8] M. Inchiosa, A. Bulsara, K. Wiesenfeld, and L. Gammaitoni, *Phys. Rev. Lett.* **A252**, 20, (1999).

[9] A.R. Bulsara, V In, et al. *Phys. Rev. E* **70**, 036103, (2004).

[10] J.A. Acebron and A.R. Bulsara and M.E. Inchiosa and W.J. Rappel, *Europhys. Lett.* **56** 354, (2001).

[11] A. Palacios, J. Aven, P. Longhini, V. In, and A. Bulsara, *Phys. Rev. E* **74**, 021122, (2006).

[12] K.G. Stawiasz and M.B. Ketchen, *IEEE Trans. Appl. Supercond.* **3**, 1808, (1993).

[13] J. Oppenländer, Ch. Häussler, and N. Schopohl, *Phys. Rev. B* **63**, 024511, (2001).

[14] Ch. Häussler, J. Oppenländer, and N. Schopohl, *J. Appl. Phys.* **89**, 1875, (2001).

[15] J. Oppenländer, Ch. Häussler, et al. *Physica C* **368**, 119, (2002).

[16] J. Oppenländer, Ch. Häussler, T. et al. *IEEE Trans. Appl. Supercond.* **13**, 771, (2003).

[17] J. Oppenländer, T. Träuble, et al. *IEEE Trans. Appl. Supercond.* **11**, 1271, (2001).

[18] J. Oppenländer, Ch. Häussler, et al. *IEEE Trans. Appl. Supercond.* **15**, 936, (2005).

[19] V K Kornev, I I Soloviev, et al. *Supercond. Sci. Technol.* **22**, 114011, (2009).

[20] Victor Kornev, Igor Soloviev, et al. *Physica C* **470**, 886, (2010).

[21] V. K. Kornev, I. I. Soloviev, et al. *IEEE Trans. Appl. Supercond.* **19**, 741, (2009).